OTC-27601-MS

Evaluation of the Intrinsic Conservatism in the Design Codes for Subsea Mudmats

B. A. M van de Riet, Mammoet; N. B. Yenigul and R. Burgers, Allseas; F. Pisanò, Delft University of Technology

Copyright 2017, Offshore Technology Conference

This paper was prepared for presentation at the Offshore Technology Conference held in Houston, Texas, USA, 1–4 May 2017.

This paper was selected for presentation by an OTC program committee following review of information contained in an abstract submitted by the author(s). Contents of the paper have not been reviewed by the Offshore Technology Conference and are subject to correction by the author(s). The material does not necessarily reflect any position of the Offshore Technology Conference, its officers, or members. Electronic reproduction, distribution, or storage of any part of this paper without the written consent of the Offshore Technology Conference is prohibited. Permission to reproduce in print is restricted to an abstract of not more than 300 words; illustrations may not be copied. The abstract must contain conspicuous acknowledgment of OTC copyright.

Abstract

Rectangular mudmat foundations for subsea structures are commonly designed according to ISO and API guidelines. However, the modern trend towards deeper waters and heavier structures is currently challenging traditional approaches to foundation design, especially in presence of particularly poor soil conditions. The intrinsic conservatism carried by design codes may not only lead to higher fabrication/installation costs, but also conflict with the operational limits of existing installation vessels.

Based on the analysis of four design cases, it is argued that ISO/API safety factors may be from 1.5 to 2.3 times as low as the predictions of elastoplastic finite element (FE) simulations. Such a conservatism is also found to considerably increase with the embedment depth, whereas the influence of the foundation aspect ratio is nearly negligible. A simple calculation example shows that the systematic use of numerical analysis in design may result in a 47% reduction of the total foundation area, and an overall decrease in fabrication costs of approximately 16%.

Introduction

Shallow mudmat foundations are widely used in offshore oil and gas developments to support subsea infrastructures, such as pipeline end terminations (PLETs), flowline end terminations (FLETs) and manifolds. A typical example is shown in Figure 1, where the main components of a pipeline infrastructure are sketched: four wellheads are connected to a hydrocarbon well and to a manifold (yellow structure in the centre) by means of jumpers, in turn linking the manifold to PLETs (grey structures).

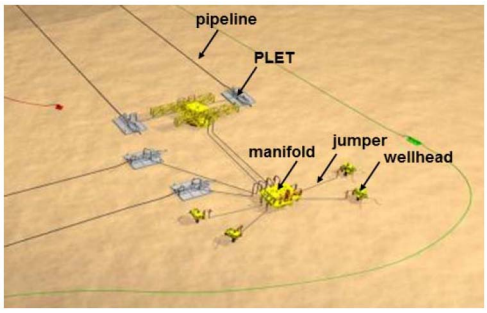

Figure 1—Overview of a pipeline infrastructure

Due to the growing demand for installations in ultra-deep waters on soft soils, substantial research is being devoted worldwide to enhance foundation design (Gourvenec and Randolph, 2003; Salgado et al., 2004; Gourvenec et al., 2006; Gourvenec, 2007; Gourvenec, 2008; Taiebat and Carter, 2010; Feng et al., 2014; Feng & Gourvenec, 2015; Dunne & Martin, 2016), and reduce the conservatism in offshore industry guidelines - such as API RP 2A-WSD (API, 2002), ISO 19901-4 (ISO, 2003) and API RP2GEO (API, 2011). Such intrinsic conservatism is magnified by the trend towards larger pipeline diameters and heavier subsea structures, and is believed to drive significant costs in terms of both fabrication and operational limits of current installation vessels. Loading amplitudes are growing higher and requiring increasing mudmat sizes, eventually hitting the installation limits of moderate-size pipe-laying vessels.

Mudmats may be classified as rectangular skirted foundations (Figure 2). At present, they are still designed based on classical foundation capacity theories, implying the use of (semi)empirical coefficients to cope with 3D effects within a plane strain (2D) framework (Feng and Gourvenec, 2014). However, the interaction among different load components (vertical-horizontal-moment) is particularly pronounced in subsea foundations, which makes the conservatism of design codes hard to assess through engineering judgement.

Figure 2—PLET structure during prior to installation (courtesy of Allseas)

In this study, 3D finite element (FE) elastoplastic calculations are performed to critically evaluate two design codes with respect to mudmat design in very soft clay. In particular, the standards ISO:19901-4 (ISO, 2003) and API RP 2A-WSD (API, 2002) are considered for two reasons: (i) they are part of Allseas' practice for mudmat design; (ii) they adopt different safety measures, based on the concepts of partial and global safety factor, respectively.

The whole process from soil characterisation to foundation analysis is encompassed on four design cases, and foundation safety factors from industry guidelines and FE analyses are compared for both partial and global safety factor approaches. Parametric studies are carried out to capture the influence on design conservatism played by the aspect ratio and the embedment depth of the mudmat.

All analytical and numerical analyses are based on the following simplifying assumptions:

- rectangular mudmat founded on soft to very soft homogeneous clay layers;
- total stress undrained analysis;
- static loading conditions (no cyclic/dynamic effects);
- no installation effects;
- deterministic design calculations and parametric analyses.

Subsea structures on multiple footing systems are not considered in this study due to the lacking guidance provided in this respect by IS0:19901-4 and API RP 2A-WSD.

The discussion is concluded by a simple calculation example showing the possible saving prospected by more accurate mudmat analysis.

Industry Design Guidelines for Subsea Mudmats

This section recalls the main features (and differences) of the design standards API RP 2A-WSD (API, 2002 - reviewed in 2014) and ISO 19901-4 (ISO, 2003). They have been selected to compare the conservatisms from two design codes as different as possible.

Safety factors

The first macroscopic difference concerns the definitions of safety factor, needed to quantify the uncertainties in the identification of loads and resistance - in geotechnical applications the latter is usually governed by the soil strength.

The API RP 2A-WSD code relies upon the so-called "global safety factor" approach, also termed "Working Stress Design" (WSD) approach. In this context, a single total safety factor γ_G is defined to reduce the resistance *(R)* and establish a "safe" balance with all external loads, namely permanent (G), variable *(Q)* and environmental *(E)*:

$$\frac{R}{\gamma_G} = G + Q + E \tag{1}$$

The API code requires γ_G larger than 2 and 1.5 for vertical bearing failure and sliding, respectively.

In contrast, the ISO 19901-4 code works according to the "partial safety factor" approach, also referred to as "Load and Resistance Factor Design" (LRFD) approach. In this alternative framework, separate safety factors are applied to reduce resistance *(γ_m)* and magnify loads *(γ_g, γ_q* and *γ_e)* - compare to Equation 1:

$$\frac{R}{\gamma_m} = \gamma_g G + \gamma_q Q + \gamma_e E \tag{2}$$

Due to the presence of all partial safety factors in Equation (2)), the ISO code requires Equation (2)) to be fulfilled as an equality, and the corresponding global safety factors must not be less than 1.

The following subsections clarify how the resistance term *R* in Equations (1)-(2) is specified within the API and ISO codes. In particular, the events of (i) vertical bearing failure and (ii) horizontal sliding are considered, while load interaction effects are handled by means of (semi)empirical correction factors. It should also be noted that this traditional approach - here maintained for consistency with industry guidelines - is being overcome by the research work on the definition of suitable vertical-horizontal-moment (VHM) failure envelopes (Taiebat and Carter, 2010; Feng et al., 2014; Vulpe et al. 2014).

Capacity equations in API RP 2A-WSD (2002)

According to the API code, the undrained vertical capacity V_{ult} of a mudmat on clay can be expressed as:

$$V_{ult} = (N_c K_c s_u + \gamma D) A' \tag{3}$$

where s_u is the undrained soil strength (constant along the depth), $N_c = 5.14$ a (plane strain) bearing capacity factor, γ the saturated soil unit weight and D the embedment depth measured from the mudline. The clay shear strength is assumed not to vary along the depth, while the coefficient K_c

$$K_c = i_c s_c d_c g_c b_c \tag{4}$$

unifies the effects of load inclination (i_c), foundation shape (s_c), embedment (d_c), sloping mudline (g_c) and mudmat inclination (b_c) - the analytical equations for the factors i_c, s_c, d_c, g_c, and b_c may be found in the original API code (API, 2002) or in van de Riet (2016). The effective base area of the mudmat is obtained by multiplying the length L and the breadth B, to be reduced as per Meyerhof (1953) in case of eccentric vertical load:

$$A' = B'L' \tag{5}$$

As for the sliding resistance, the following equation is considered in this study:

$$H_{ult} = H_{ult1} + H_{ult2} + H_{ult3} = BLs_u + 2LDs_u + 4BDs_u \tag{6}$$

in which the original term H_{ultl} is complemented by the terms H_{ult2} (side adhesion) and H_{ult3} (active/passive-like earth pressure) to include the typical extra capacity of skirted mudmats. Obviously, sliding checks with only $H_{ult} = H_{ultl}$ would be highly overconservative.

Capacity equations in ISO 19901-4 (2003)

The ISO counterparts of the API Equations (3)-(6) read as follows:

$$V_{ult} = \left[\left(N_c s_{u0} + \frac{kB\prime}{4}\right)\frac{FK_c}{\gamma_m} + \gamma' D\right]A' \tag{7}$$

$$K_c = 1 + s_c + d_c - i_c \tag{8}$$

$$A' = B'L \tag{9}$$

$$H_{ult} = H_{ult1} + H_{ult2} + H_{ult3} = BL\frac{s_{u,ave}}{\gamma_m} + 2LD\frac{s_{u,ave}}{\gamma_m} + 4BD\frac{s_{u,ave}}{\gamma_m} \tag{10}$$

Other than the adoption of the partial safety factor approach, it is also worth noting that:

- Equation (7)) allows for a linear distribution of the undrained soil strength, where s_{u0} denotes the strength at the mudline and k the depth gradient. The correction factor F accounts for the degree of soil inhomogeneity;
- the ISO code does also include a simpler version of Equation (7)) with constant s_u, here not taken into account;
- the correction factor K_c results from the additive - not multiplicative - terms provided in ISO (2003) and van de Riet (2016) (Equation (8));
- as for the API case, the sliding resistance of embedded mudmats is calculated here by enhancing the original equation based on H_{ult1} exclusively. In Equation (10)) $s_{u\ ave}$ is the average soil strength over the 0 — D depth range.

Design Case Studies

The conservatism in design standards is here investigated by critically reconsidering four Allseas design cases from two pipeline projects in the Mediterranean Sea (cases 1-2) and off the coasts of Brazil (cases 3-4). In what follows the main information relevant to the four situations is summarised in terms of site characterisation and soil parameters, foundation geometry and load combinations.

The subsea foundations considered for the first project are a 16 inch PLET and a 10 inch dualhub FLET, installed at 1650 and 1700 metres water depths, respectively. During the site investigation, cone penetration tests (CPTs) were performed and soil samples retrieved. The geotechnical survey revealed the presence of two clayey layers, with an extremely soft top layer containing shell fragments and a slightly firmer layer underneath.

As for the second project, a 20 inch PLET (2200 metres water depth) and a 24 inch PLET (650 metres water depth) are considered. During the geotechnical investigation, CPTU and T-Bar tests were performed along the pipeline route and about 100 soil samples extracted through either a vibrocore or a Kullenberg sampler. Very loose to dense sands over clay were identified at the shallowest sections of the route, whereas very soft clays were found at deeper locations.

Figure 3 depicts the four undrained shear strength data for the soft soils at each project site. Other soil data not strictly needed for the analyses being presented (e.g. water content, Atterberg limits, etc.) are not reported for the sake of brevity. All reported soil data should be regarded in light of the following considerations:

- the apparent scatter in all s_u profiles is due to spatial inhomogeneity (data are from different locations, possibly kilometres away from the mudmats) and different testing procedures. These latter include CPT(U), torvane, hand- and lab-vane, unconsolidated undrained (UU) triaxial tests;
- only s_u values from locations relatively close to the structures were used to derive engineering soil parameters;
- geotechnical surveys returned s_u values within the typical range for soft clayey sediments. Figure 3 also illustrates two possible interpretations of the strength data, namely in the form of linear and constant strength profiles. The latter is needed for use in Equations (3)-(6), which do not allow for depth-varying undrained strength.

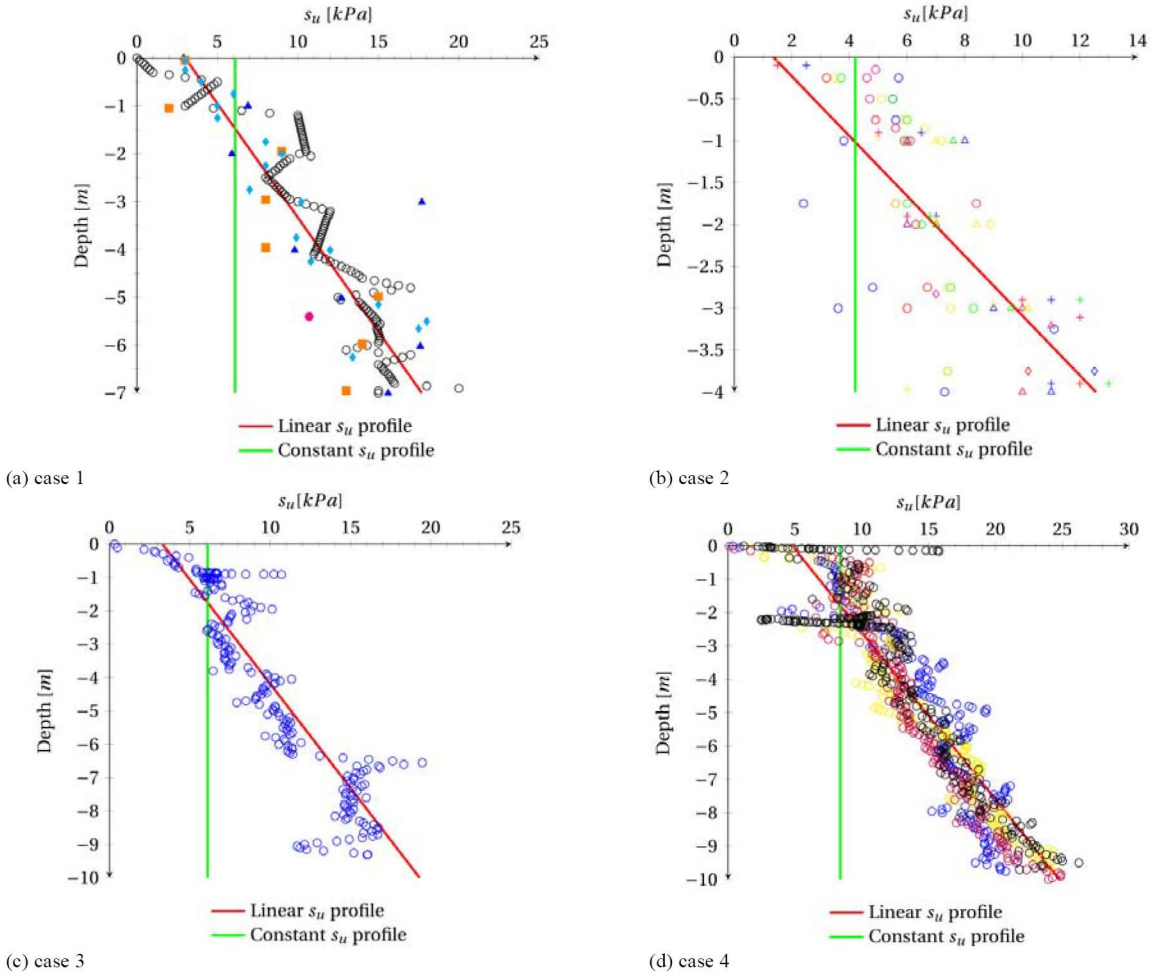

Figure 3—Soil strength data/profiles for the four design cases

It should be noted that obtaining constant values from the strength profiles in Figure 3 is to some extent arbitrary, so a FE-based procedure had to be conceived for this purpose. After determining linear s_u profiles via the regression of site data, equivalent constant s_u values were numerically identified to keep the vertical capacity and the failure mechanism as those resulting from linear s_u profiles (van de Riet, 2016).

All soil parameters for both analytical and FE calculations are listed in Table 1 (as no specific measurements were available, the E/s_u ratio was assumed based on standard practice/literature). Input data concerning geometries and load combinations are provided in Table 2 and 3, respectively.

Table 1—Soil parameters in the four design cases

Parameter	Symbol	Unit	Case 1	Case 2	Case 3	Case 4
Saturated unit weight	Y	[kN/m^3]	15.6	14.5	14.5	16
Shear strength at the mudline	S_{u0}	[kPa]	3	1.35	3.3	4.8
Shear strength gradient	k	[kPa/m]	2.1	2.8	1.6	2
Representative constant shear strength	s_u	[kPa]	6.1	4.2	6.1	8.4
Poisson's ratio	V	[-]	0.495	0.495	0.495	0.495
Young's modulus to shear strength ratio	E/s_u	[-]	350	350	300	300

Table 2—Mudmat geometry in the four design cases

Foundation Size	Symbol	Unit	Case 1	Case 2	Case 3	Case 4
Length	L	[m]	11	8.9	13	13
Width	B	[m]	10	8.6	10	10
Embedment	D	[m]	0.3	0.3	0.5	0.4
Aspect ratio	B/L	[-]	0.91	0.97	0.77	0.77

Table 3—External load combinations in the four design cases (xy is the mudmat plane, z the vertical axis)

Load Component	Unit	Case 1	Case 2	Case 3	Case 4
F_x	[kN]	37	−58	−45	−74
Fy	[kN]	−42	−63	64	125
F_z	[kN]	−887	−627	−1190	−1229
M_x	[kNm]	1308	714	−1490	−1420
My	[kNm]	203	−357	1064	889
M_z	[kNm]	235	203	472	707

FE Analysis of Conservatism in Standard Design Practice

This section reports a re-examination of the above design cases to identify, by comparison to FE analyses, the conservatism in design codes. Then, the effects on conservatism of the mudmat aspect ratio and embedment

are parametrically investigated, as in practice these are the two main free parameters for designers. Design conservatism is here explored with reference to vertical bearing failure and sliding exclusively, as these are the only two failure modes regarded by the API and ISO guidelines. Conversely, the critical assessment of displacement predictions as per design standards is beyond the scope of this work.

3D FE modelling

All FE simulations have been performed through PLAXIS 3D models featuring the following characteristics:

- total stress, elastoplastic, associative Tresca soil model (parameters in Table 1);
- the soil domain is discretised into 10-node tetrahedral elements with local mesh refinement around the foundation area (Figure 4a). Preliminary mesh sensitivity analyses have been carried out to compromise computational burden and accuracy;
- as steel mudmats are much stiffer than the underlying soft sediments, the foundations is modelled in all cases as a rectangular rigid body (Figure 4b) (Horikoshi & Randolph, 1997) - including mudmat, skirts and the soil contained. This choice is appropriate as long as the number of skirts is enough to prevent failure within the inner soil (Acosta-Martinez et al., 2008; Mana et al., 2012);
- no strength reduction is applied at the soil-mudmat interfaces (Figure 4b), in accordance with the design standards considered;

(a) Example of a FE mesh employed for numerical simulations (b) Mudmat rigid body with surrounding interfaces

Figure 4—PLAXIS 3D FE model

FE safety factors have been determined by adopting the so-called "load increasing method", that is by applying load step increments until the attainment of the ultimate load *Fult,* either vertical $(F_{ult} = V_{ult})$ or horizontal $(F_{ult} = H_{ult})$. While the relevant load component (vertical or horizontal) is monotonically increased, the other components in Table 3 are kept unaltered until failure. Finally, the FE safety factor is calculated as the ratio between F_{ult} and the corresponding initial value F_{in} from Allseas' structural design reports:

$$SF_{FE} = \frac{F_{ult}}{F_{in}} \tag{11}$$

Unfactored input parameters have been used for comparison to the API code, whereas partial safety factors have been applied to input parameters in order to make FE and ISO results comparable. In agreement with Allseas' previous analyses, only static loads have been considered in this study. It should be also mentioned that the API/ISO design codes do not provide any specific guidance on cyclic and dynamic loading conditions.

Retrospection of design cases

Figure 5 provides a visual comparison between the API/ISO safety factors and their FE counterparts for the four designs. In particular, the soil properties and geometrical/loading parameters in Tables 1-3 have been adopted to point out how different safety levels may be assessed through design standards and FE simulations.

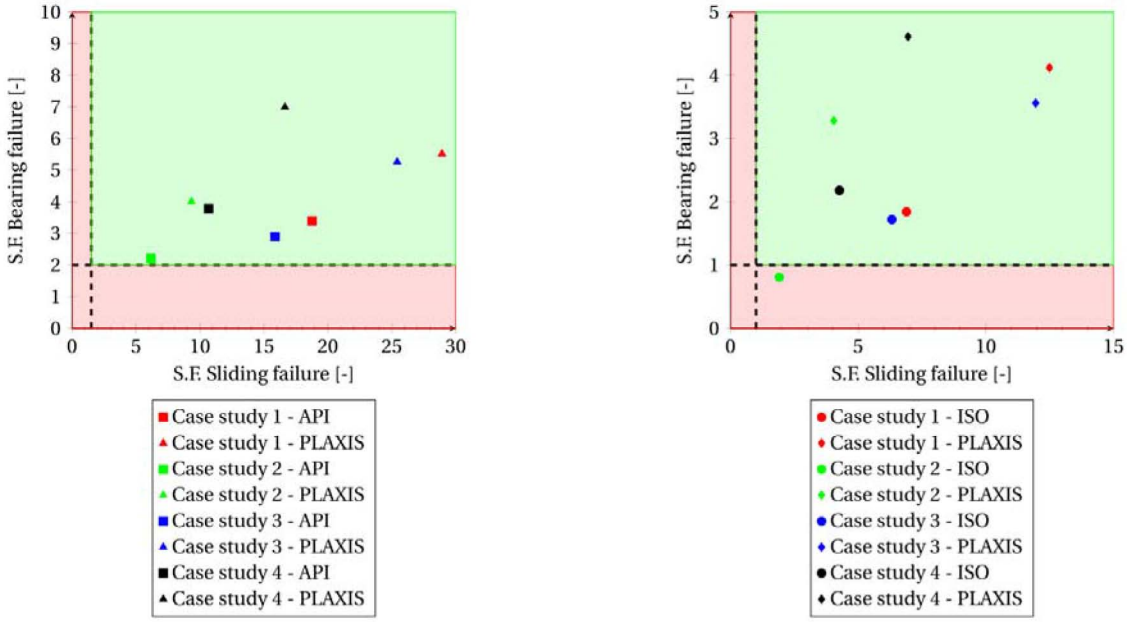

(a) API vs FE (global safety factor approach)

(b) ISO vs FE (partial safety factor approach)

Figure 5—Comparison between the safety factors from the design codes and PLAXIS FE calculations

Figure 5 gives a clear impression of the conservatism featured by both design codes. Such conservatism is quite uniform over the four design cases and applies to both bearing and sliding failures. While previous designs were kept relatively close to standard safety limits (red-shaded zones should not be approached), FE results show that, with the same input information, all mudmats work in better conditions than predicted. This is a direct consequence of the abrupt simplifications on the effects of embedment and loading interactions - such as the effect of moments on the bearing capacity, or of torsion on the sliding limit (Murff et al., 2010; Feng et al., 2016).

Parametric studies

In order to better quantify the conservatism in the API/ISO codes, the results of parametric analyses are displayed in Figures 6-9 in terms of API/ISO-to-FE safety factor ratios for a meaningful range of aspect ratios (from 0.5 to 1) and embedment depths (from 0 to 1 metre).

The results in Figures 6-9 encompass typical practical situations (including the above design cases), and show that the FE safety factors for bearing and sliding failures are consistently from 1.5 to 2.3 times higher than from design standards.

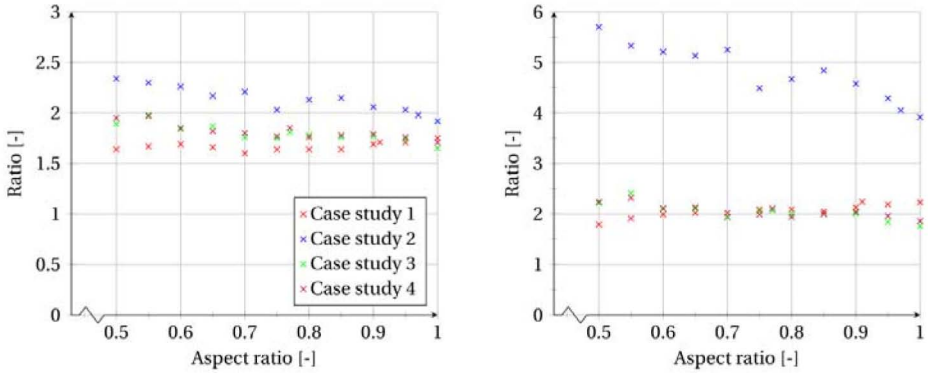

Figure 6—Influence of the mudmat aspect ratio on the API-to-FE (left) and ISO-to-FE (right) safety factor ratios for vertical bearing failure

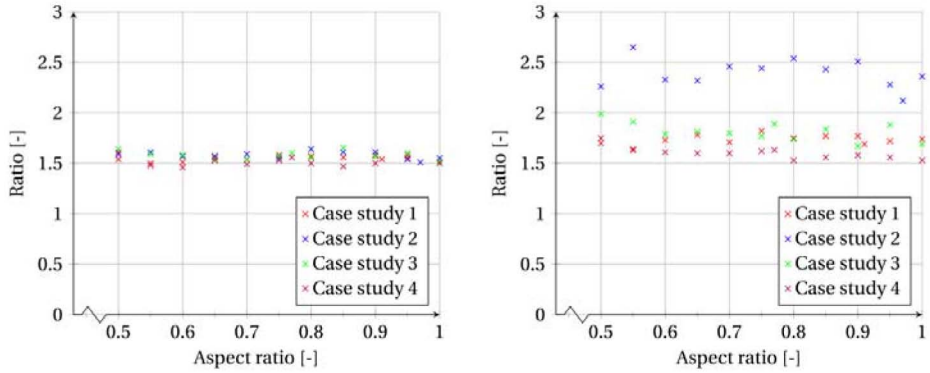

Figure 7—Influence of the mudmat aspect ratio on the API-to-FE (left) and ISO-to-FE (right) safety factor ratios for sliding failure

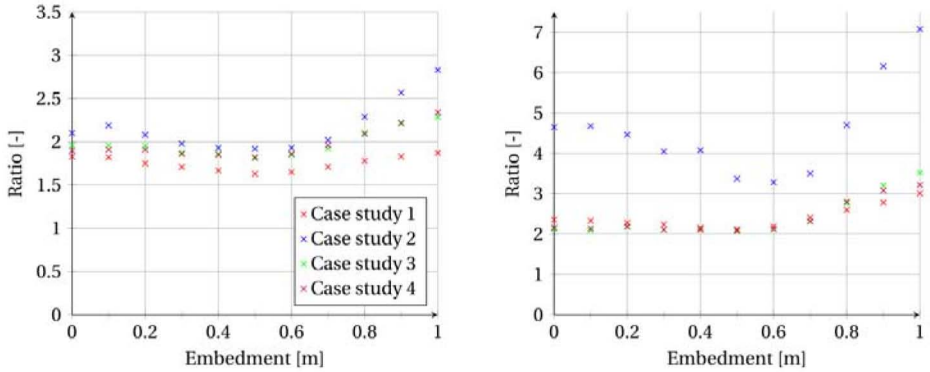

Figure 8—Influence of the mudmat embedment on the API-to-FE (left) and ISO-to-FE (right) safety factor ratios for vertical bearing failure

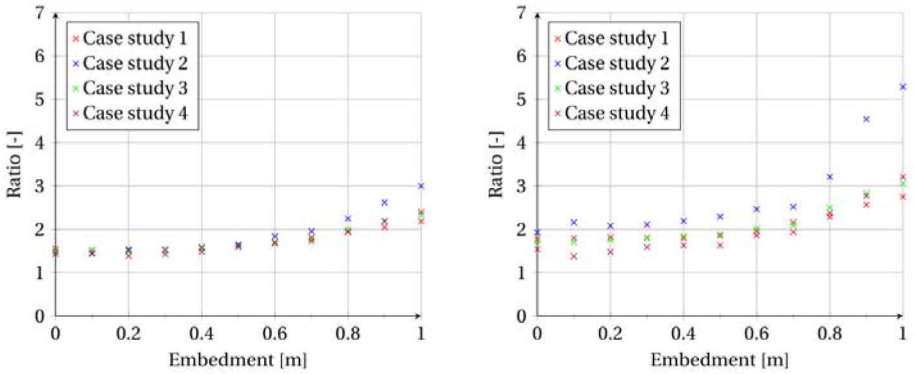

Figure 9—Influence of the mudmat embedment on the API-to-FE (left) and ISO-to-FE (right) safety factor ratios for sliding failure

The following observations arise from the outcomes of the parametric studies:

- the influence on conservatism of the mudmat aspect ratio is quite limited, especially for sliding failure;
- conservatism tends to progressively increase at larger embedment depths;
- the design case 2 features the highest conservatism, somewhat out of the range spanned by the other three cases. This finding is more evident for ISO safety factors.

A plausible explanation to the third point stems from a closer inspection of the load inclination factor in Equation (8):

$$i_c = 0.5\left[1 - \sqrt{1 - \frac{H}{B' L s_{u0}/\gamma_m}}\right] \tag{12}$$

whence i_c values equal to 0.087, 0.341, 0.083 and 0.119 result for the design cases 1 to 4, respectively. Due to the lower soil strength (Table 1) and foundation area (Table 2), the ISO formulae return in case 2 the highest inclination factor and a significant margin of safety against collapse (see also Figure 5).

The API/ISO-to-FE safety factor ratios quantify the "mechanical ignorance" in design standards generated by simplified foundation theories. It is therefore expected that the degree of conservatism grows higher when the interaction between load components (e.g. substantial load inclination) or the geometrical set-up (e.g. embedment) move farther from the ideal conditions assumed by those theories. Nonetheless, the present practical exercise gives a clear picture about how much conservatism is embedded into traditional design calculations, and may provide useful arguments to designers struggling with geotechnical and economical requirements.

Additional sources of conservatism may arise from more sophisticated soil modelling, including e.g. the effects of pore pressure, prefailure hardening, strength anisotropy, cyclic loading, etc. These aspects have not been investigated in this study to allow fair comparisons between standard and FE calculations.

Simplified Analysis of Cost Reduction

The above results highlight the significant conservatism characterising the industry guidelines for mudmat design, and point out a remarkable potential for optimisation and cost reduction. Such a potential is discussed hereafter by reconsidering the first design case in light of the identified conservatism.

A typical PLET can be regarded as a subsea structure formed by piping and structural components. The piping component consists of pipelines, valves and connectors (Figure 10a), while structural components include mudmat, yoke, piping frame and piggy back supports (Figure 10b). The present cost reduction analysis relies upon the following assumptions (and the exchange rate € 1= $ 1.07385):

- the fabrication cost of piping components is driven by the type and number of welds;

- the costs for piping fabrication are not affected by geotechnical design;
- the costs for the fabrication of structural components are determined by the unit rates of steel structures. These rates evolve in time due to steel price, mudmat complexity and market situation. A unit rate of € 7.5 *(*~ $ 8) per kilogram is here assumed;
- only the amount of mudmat steel - not of other structural steel - is affected by geotechnical design.

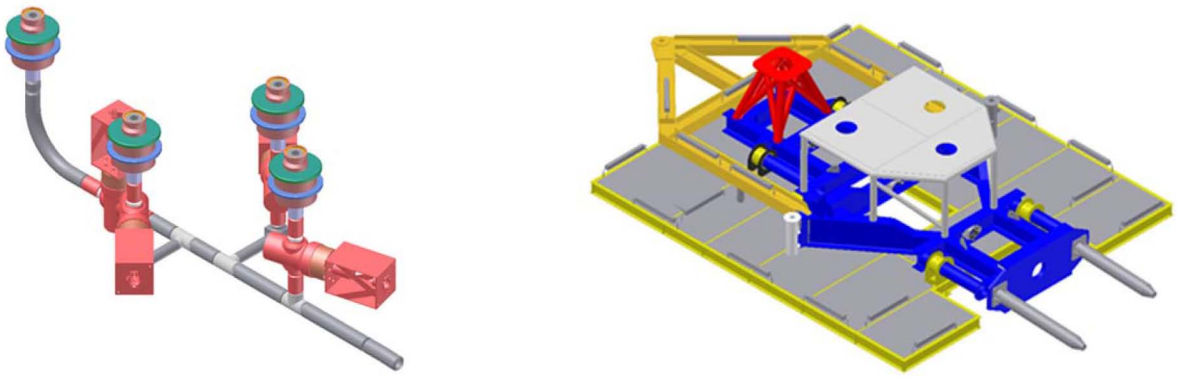

(a) piping components (b) structural components

Figure 10—Components of a typical PLET

The above analyses foster cost reduction through mudmat resizing, with no immediate effects on the other cost factors. Based on the API guidelines, the following specifications were set at Allseas for the design case 1 - here considered for quantitative calculations:

- width: 10 m, length: 11 m, embedment: 0.3 m;
- equal weight of 19.5 tons for mudmat and structural steel.
- fabrication costs for structural steel: € 292.500 (≈ $ 314.101), estimated cost of piping components: € 146.250 (≈ $ 157.051), total: € 438.750 (≈ $ 471.152);

FE results are now used to reduce width and length of the mudmat up to the attainment of the same API safety factor for bearing failure (governing mode), while the 0.3 m is kept unmodified. The following new design settings are obtained accordingly:

- width: 7.3 m, length: 8 m, embedment: 0.3 m;
- reduction in foundation area: 47%, new mudmat fabrication cost: € 77.500 (≈ $ 83.223);
- cost reduction for fabrication: € 68.750 (≈ $ 73.827) – 16% of the previous total.

The significance of such cost reduction could be further emphasised by considering operational installation costs. If improved smaller mudmats can be designed (though not smaller than required for practical functionality), then a wider time window for installation could be enabled. Savings even higher than for fabrication may be achieved by optimising installation operations (e.g. lower waiting time for installation vessels) through foundation design.

Concluding Remarks

The conservatism embedded in the API RP 2A-WSD and ISO 19901-4 ISO codes for subsea mudmats was investigated by comparison to 3D elastoplastic FE computations. For this purpose, four design cases - concerning mudmats on soft clay - were reconsidered by evaluating the safety factor ratios API-to-FE (global safety factor approach) and ISO-to-FE (partial safety factor approach) for both vertical bearing failure and sliding. Special care was devoted to analyse FE mesh effects and minimise unavoidable discretization errors (usually in the form of overestimated capacities).

Results showed that the API/ISO-to-FE safety factor ratios for vertical and sliding failures lie in the range from 1.5 to 2.3 in most cases, and indicate that significant conservatism is embedded in industry design guidelines. In particular, the ISO code seemed to be the most conservative in the four situations considered, although general conclusions may hardly be drawn due to the different safety philosophies adopted by the two codes (global vs partial). The identified conservatism was found in all cases to be negligibly affected by the aspect ratio of the mudmat, whereas the embedment ratio of the foundation played a substantial role - especially when in excess of 0.5 metres.

This study confirmed that ignoring coupling effects among different loading components is excessively safe, and lead to pronounced cost ineffectiveness in mudmat design. An impression of the expected saving on the fabrication costs for structural steel material costs was finally provided, showing remarkable cost reduction (in the order of 16%) for the one case taken into consideration.

Acknowledgements

B.A.M. van de Riet thanks Allseas (Delft, Netherlands) for hosting his MSc graduation project in cooperation with TU Delft.

References

Acosta-Martinez, H. E., Gourvenec, S. M., & Randolph, M. F. (2008). An experimental investigation of a shallow skirted foundation under compression and tension. *Soils and Foundations*, **48**(2), 247–254.

API (2002) Recommended Practice for Planning, Designing and Constructing Fixed Offshore Platforms - Working Stress Design, 21st edition, *Errata and Supplement 1*, American Petroleum Institute, Washington (DC), USA

API (2011) *Recommended Practice 2GEO Geotechnical and Foundation Design Considerations*, 1st Edition, American Petroleum Institute, Washington (DC), USA.

Dunne, H. P., & Martin, C. M. (2016). Capacity of rectangular mudmat foundations on clay under combined loading. *Geotechnique*, 1–13.

Feng, X., & Gourvenec, S. (2014). A Method for Predicting Six Degrees-of-Freedom Ultimate Limit State of Subsea Mudmats. In ASME 2014 33rd International Conference on Ocean, Offshore and Arctic Engineering (pp. V003T10A004–V003T10A004). American Society of Mechanical Engineers.

Feng, X., Randolph, M. F., Gourvenec, S., & Wallerand, R. (2014). Design approach for rectangular mudmats under fully three-dimensional loading. *Geotechnique*, **64**(1), 51–63.

Feng, X., & Gourvenec, S. (2015). Consolidated undrained load-carrying capacity of subsea mudmats under combined loading in six degrees of freedom. *Geotechnique*, **65**(7), 563–575.

Feng, X., Randolph, M. F., & Gourvenec, S. (2016). An analytical solution for the undrained horizontal-torsional resistance of mudmats. *Geotechnique*, 113.

Gourvenec, S., & Randolph, M. (2003). Effect of strength non-homogeneity on the shape of failure envelopes for combined loading of strip and circular foundations on clay. *Geotechnique*, **53**(6), 575–586.

Gourvenec, S., Randolph, M., & Kingsnorth, O. (2006). Undrained bearing capacity of square and rectangular footings. *International Journal of Geomechanics*, **6**(3), 147–157.

Gourvenec, S. (2007). Shape effects on the capacity of rectangular footings under general loading. *Geotechnique*, **57**(8), 637–646.

Gourvenec, S. (2008). Effect of embedment on the undrained capacity of shallow foundations under general loading. *Geotechnique*, **58**(3), 177–186.

Horikoshi, K., & Randolph, M. F. (1997). On the definition of raft-soil stiffness ratio for rectangular rafts. *Geotechnique*, **47**(5).

ISO 19901-4 (2003) Petroleum and natural gas industries —specific requirements for offshore structures — Part 4: Geotechnical and foundation design considerations, 1st Edition. *International Standardisation Organisation*.

Mana, D. S., Gourvenec, S., & Martin, C. M. (2012). Critical skirt spacing for shallow foundations under general loading. *Journal of Geotechnical and Geoenvironmental Engineering*, **139**(9), 1554–1566.

Meyerhof, G.G. (1953). The bearing capacity of foundations under eccentric and inclined loads, Proceedings of the 3rd International Conference on Soil Mechanics and Foundation Engineering, Zurich (Switzerland), Vol. **1**, pp. 440–445.

Murff, J. D., Aubeny, C. P., & Yang, M. (2010). The effect of torsion on the sliding resistance of rectangular foundations. In Proceedings of the 2nd International Symposium on Frontiers in Offshore Geotechnics, Perth (Australia), pp. 439–443.

van de Riet, B.A.M. (2016). *Shallow foundations for subsea structures: a comparison between design codes and numerical analysis*, MSc dissertation, Delft University of Technology (The Netherlands)

Salgado, R., Lyamin, A. V., Sloan, S. W., & Yu, H. S. (2004). Two-and three-dimensional bearing capacity of foundations in clay. *Geotechnique*, **54**(5), 297–306.

Taiebat, H. A., & Carter, J. P. (2010). A failure surface for circular footings on cohesive soils. *Geotechnique*, **60**(4), 265–273.

Vulpe, C., Gourvenec, S., & Power, M. (2014). A generalised failure envelope for undrained capacity of circular shallow foundations under general loading. *Geotechnique Letters*, **4**, 187–196